Received March 31, 2020, accepted April 24, 2020, date of publication April 29, 2020, date of current version May 15, 2020.

Digital Object Identifier 10.1109/ACCESS.2020.2991163

Simple Coupled-Line Tunable Bandpass Filter With Wide Tuning Range

XIAOXIAO CHEN, YONGLE WU, (Senior Member, IEEE), YUHAO YANG, AND WEIMIN WANG, (Member, IEEE)

School of Electronic Engineering, Beijing University of Posts and Telecommunications, Beijing 100876, China

Corresponding author: Yongle Wu (wuyongle138@gmail.com)

This work was supported in part by the Beijing Natural Science Foundation under Grant JQ19018, and in part by the National Natural Science Foundation of China under Grant 61971052.

ABSTRACT In this paper, a tunable bandpass filter using coupled line with a wide tuning range is proposed. The proposed filter has a simple structure which is composed of a coupled-line section and two pairs of varactors. Meanwhile, simultaneously tuning on bandwidth and center frequency are introduced by varactors. The tunability is mainly realized by varactors connected to one end of the coupled line and varactors between ports and coupled line provide an impedance matching. A theoretical analysis is presented to illustrate the tunability by using even- and odd-mode theory. Additionally, the detailed effect of the two types of varactors is researched, respectively. To verify the concept, a prototype is designed, fabricated, and measured. The transmission zero exhibited in measurement is introduced by bias circuits. The measured results show that the tunable bandpass filter achieves a tunable center frequency of 0.494-1.257 GHz (87.15%) and a 3-dB bandwidth of 0.282-0.943 GHz (334%).

INDEX TERMS Bandpass filter, coupled line, tunable filter, wide tuning range.

I. INTRODUCTION

Reconfigurable or high-performance microwave devices, such as power dividers [1]–[3], phase shifters [4]–[7], couplers [8]–[10], and filters [11]–[33], are extensively studied in past several years. Due to the reconfigurability, these key components used in modern wireless communication systems are capable to realize the agile frequency to support different standards, as well as reduce the size and complexity of systems. Thus, the flexibility and applicability of systems will eventually be realized.

As indispensable components, tunable filters are widely used in modern wireless communication systems because of their selectivity. From general perspective, tunable filters involve the following categories, including tunable bandstop filters [31], low-pass filters [32], high-pass filters [33], and bandpass filters (BPFs) [11]–[19], [21]–[29]. Moreover, the tunable BPFs with widespread applications can be classified as filters with tuning frequency with constant absolute bandwidth [15], [19], controllable operating bandwidth with fixed center frequency [29], and both bandwidth and frequency reconfigurable [16], [17]. Various methods can be employed to achieve the tunability of bandpass filters, such as varactors [21], PIN diodes [27], microelectromechanical systems (MEMS) devices [28], and so on. As far as varactors are concerned, many structures have been adopted to implement tunability, including the modified parallel-coupled line [11], the comb line [12], and the coupled line resonator [13], etc. However, these agile frequency filters cannot provide a relatively wide tuning range, which simultaneously need high bias voltages, multiple varactors, or complicated structures. A tunable BPF using short parallel-coupled lines is presented in [22], which includes six varactors and three DC voltages. However, a better performance on tuning range can be obtained with a simpler structure, thus decreasing design complexity of bias circuits. Such a design can reduce the cost and increase the reliability, which is more applicable in modern multi-band communications.

In [4], the author presents a tunable reflection phase shifter based on short section of coupled lines. Then, a phase reconfigurable microwave power divider is proposed in [34]. Through loaded with reflection-type loads, coupled line can be tunable as an effective variable length transmission line (TL) approximately. Based on these fundamental

The associate editor coordinating the review of this manuscript and approving it for publication was Haiwen Liu.

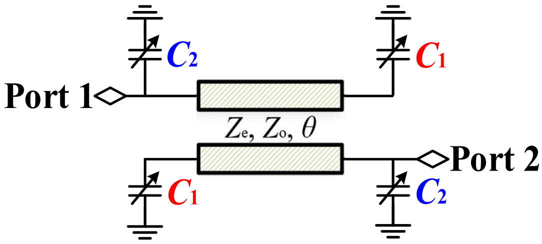

FIGURE 1. **Schematic diagram of the tunable BPF.**

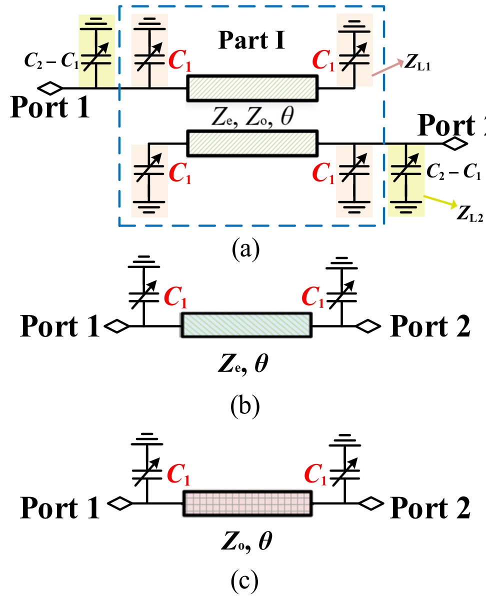

FIGURE 2. **(a) Equivalent circuit of the tunable BPF. (b) The even-mode equivalent circuit of Part I. (c) The odd-mode equivalent circuit of Part I.**

theories, a coupled line-based coupler with simultaneously tunable phase and frequency is displayed in [9]. The proposed varactor loaded coupled-line structure is introduced between two quarter-wavelength coupled-line sections to implement the simultaneously phase and frequency tunable coupler. Enhancement in both bandwidth and phase tunable range has been come true. In addition, only using coupled lines loaded with impedances can design the high-power amplifier [35] and dual-band DC-block transformer [36]. Furthermore, novel rat-race couplers based on coupled lines demonstrate tunable frequency with unequal power division [37]. Besides, the reconfigurable idea can also be applied in antenna [38] to achieve polarization diversity, by adopting a reconfigurable feeding network using a quasi-lumped coupler and PIN diodes. Therefore, a simple coupled-line BPF with wider tuning range is possible to be a part of microwave devices to achieve superior performance. Different from the previous bandpass filters [40], [41], this article focuses on the wider tuning range on bandwidth and frequency with simple coupled-line structure.

In this paper, a tunable BPF using a coupled line with a wide tuning range is proposed and analyzed based on the work [34]. Because of the introduced tunable capacitors, a relatively wide tuning range and preferable impedance matching are achieved. By the even- and odd-mode analysis approach, the equivalent circuits of the design are analyzed thoroughly. As ideal results demonstrate, the design realizes a shift of the center frequency (0.663-1.581 GHz, 81.82%) and bandwidth (345-838 MHz, 243%). For verification, a prototype is modeled, simulated, manufactured, and measured. The experimental results indicate the proposed BPF achieves the tunability under three different states, yielding a tuning frequency range of 87.15%. Beside the introduction, theoretical analysis and parameters study are presented in section II. In section III, the simulated and measured results are displayed and discussed. At the end, conclusions of the design are exhibited in section IV.

II. THEORETICAL ANALYSIS

A. EVEN- AND ODD-MODE ANALYSIS

Fig. 1 shows the schematic diagram of the proposed tunable BPF, which consists of a section of coupled line loaded with two types of tunable capacitors. Through connecting tunable capacitors to the end of the coupled line, the frequency tunability is introduced.

To analyze the performance of the structure, the even- and odd-mode analysis method is utilized. The equivalent circuits of the tunable BPF displayed in Fig. 2(a) simplifies the analysis of asymmetrical structure, through adding two loads Z_{L1} which are the impedance of loaded varactors C_1 [22], [34]. To eliminate the effect of the added Z_{L1}, $-Z_{L1}$ are also implemented. Z_{L2} represents the impedance of loaded varactors $-C_1$ and C_2. The even- and odd-mode equivalent sub-circuits of Part I are presented in Fig. 2(b) and Fig. 2(c).

For Part I, the impedance matrix can be extracted as a function of even- and odd-mode input impedances and A element of $ABCD$ matrix

$$Z_{11} = Z_{22} = \frac{(Z_{\text{ine}} + Z_{\text{ino}})}{2}, \tag{1a}$$

$$Z_{21} = Z_{12} = \frac{(Z_{\text{ine}}/A_{\text{e}} - Z_{\text{ino}}/A_{\text{o}})}{2}, \tag{1b}$$

where Z_{ine} and Z_{ino} are the even- and odd-mode input impedance of Part I, Z_{ij} ($i, j = 1, 2$) is the two-port matrix impedance of the coupled line, and A_{e} and A_{o} are A elements of even- and odd-mode $ABCD$ matrix.

Z_{ine} and Z_{ino} can be calculated as:

$$Z_{\text{ine}} = \frac{Z_{\text{e}}Z_{\text{L1}}(Z_{\text{L1}} + jZ_{\text{e}}\tan\theta)}{2Z_{\text{e}}Z_{\text{L1}} + j(Z_{\text{e}}^2 + Z_{\text{L1}}^2)\tan\theta}, \tag{2}$$

$$Z_{\text{ino}} = \frac{Z_{\text{o}}Z_{\text{L1}}(Z_{\text{L1}} + jZ_{\text{o}}\tan\theta)}{2Z_{\text{o}}Z_{\text{L1}} + j(Z_{\text{o}}^2 + Z_{\text{L1}}^2)\tan\theta}, \tag{3}$$

$$Z_{\text{L1}} = \frac{1}{j\omega C_1}. \tag{4}$$

A_{e} and A_{o} can be written as:

$$A_{\text{e}} = \cos\theta + \frac{jZ_{\text{e}}\sin\theta}{Z_{\text{L1}}}, \tag{5}$$

$$A_{\text{o}} = \cos\theta + \frac{jZ_{\text{o}}\sin\theta}{Z_{\text{L1}}}. \tag{6}$$

TABLE 1. Relationships between C_1 (C_2) and tuning range (Z_e = 100 Ω, Z_o = 48.6 Ω, and θ = 55° at f_0 = 1 GHz).

f_c (GHz)	0.78	0.89	1.09	1.18	1.3
C_1 (pF), C_2 =4 pF	10.80	6.02	3.15	2.50	1.40
f_c (GHz)	0.90	0.95	1.01	1.02	1.02
C_2 (pF), C_1 =4 pF	6.5	6	5	4	3

By using the transfer formulas between *ABCD* matrix and *Z* matrix, the *ABCD* matrix of Part I can be expressed as:

$$A_1 = \frac{A_o A_e (Z_{ine} + Z_{ino})}{A_o Z_{ine} - A_e Z_{ino}}, \tag{7a}$$

$$B_1 = \frac{(Z_{ine} + Z_{ino})^2 - (Z_{ine}/A_e - Z_{ino}/A_o)^2}{2(Z_{ine}/A_e - Z_{ino}/A_o)}, \tag{7b}$$

$$C_1 = \frac{2A_o A_e}{A_o Z_{ine} - A_e Z_{ino}}, \tag{7c}$$

$$D_1 = A_1. \tag{7d}$$

The *ABCD* matrix of whole circuit can be described by

$$\begin{pmatrix} A & B \\ C & D \end{pmatrix} = \begin{pmatrix} 1 & 0 \\ 1/Z_{L2} & 1 \end{pmatrix} \begin{pmatrix} A & B \\ C & D \end{pmatrix}_1 \begin{pmatrix} 1 & 0 \\ 1/Z_{L2} & 1 \end{pmatrix}, \tag{8}$$

$$Z_{L2} = \frac{1}{j\omega(C_2 - C_1)}. \tag{9}$$

The input admittance Y_{in} can be derived from the equation

$$Y_{in} = \frac{CZ_L + D}{AZ_L + B}, \tag{10}$$

where Z_L denotes the load impedance. In addition, the value of Z_L is 50 Ω.

The resonant frequency can be determined by

$$\text{Im}\,[Y_{in}] = 0. \tag{11}$$

Herein, the relationship between center frequency f_c and tunable capacitors can be calculated which are listed in TABLE 1. It is worth noting that considering the impedance matching, the tuning range of C_2 are limited from 3-6.5 pF. The details about impedance matching are shown in the Section-B of parameters analysis.

B. PARAMETERS ANALYSIS

In this section, the specific influence of C_1 and C_2 on tunability of the tunable BPF are discussed, separately. For demonstration, we choose Z_e = 100 Ω, Z_o = 48.6 Ω, and $\theta = 55°$ at f_0 = 1 GHz. Fig. 3 depicts $|S_{11}|$ and $|S_{21}|$ tuned by C_1 (C_2) with fixed C_2(C_1). The simulations are accomplished using Advanced Design System (ADS) software.

It can be observed that when C_2 is fixed, C_1 primarily affects the operating frequency of the design in Fig. 3(a), and C_2 has the main impact on the impedance matching while C_1 is fixed, as demonstrated in Fig. 3(b). Moreover, similar with the performance of $|S_{11}|$ for C_1 and C_2, the curves of $|S_{21}|$ also verify what roles C_1 and C_2 play in the performance of the tunable BPF. It is seen that when the tunable varactor C_1 changes from 1 pF to 10 pF with C_2 = 4 pF, the operating frequency varies obviously from a high frequency to a low frequency. Otherwise, the upper band of $|S_{21}|$ extends to be steep in the upward tuning process of C_2 when C_1 is fixed to 4.0 pF.

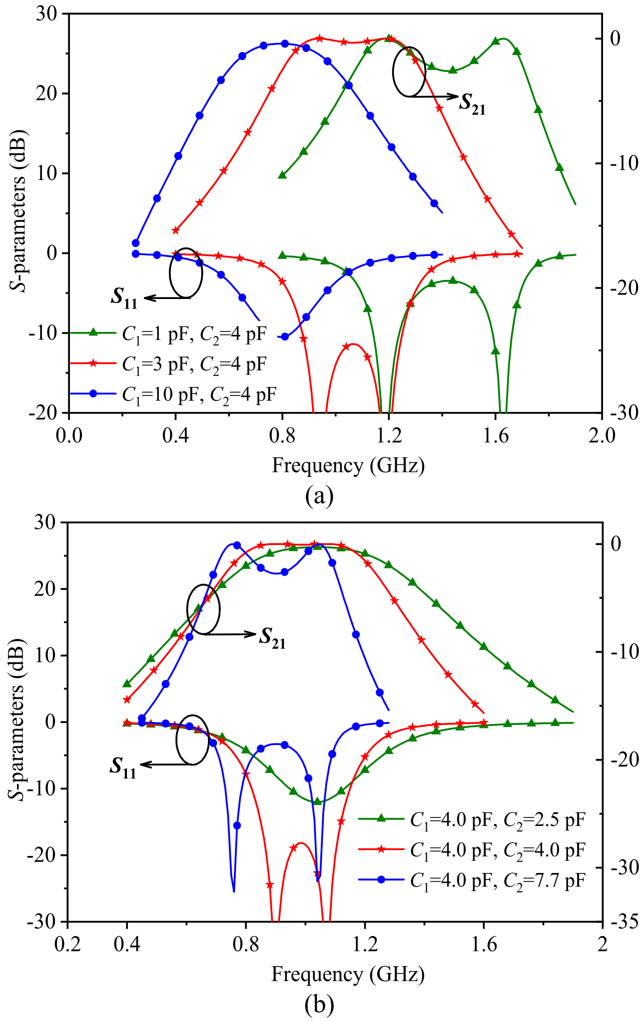

FIGURE 3. The theoretical *S*-parameter curves of the proposed tunable BPF. (a) Varied C_1 with fixed C_2. (b) Varied C_2 with fixed C_1.

By optimizations of these two types varactors, the optimized theoretical curves of proposed tunable BPF are displayed in Fig. 4. In the simulation of theoretical analysis, the return losses are better than 20 dB, and complete with a center frequency shift of 81.82% and bandwidth of 243%, as shown in Fig. 4(a). From what are plotted in Fig. 4(b), it can be seen that the upper band of $|S_{21}|$ extends towards high frequency, which is consistent with above analyses.

The designed tunable bandpass filters can be extended to higher-order filter via loading additional varactors. As shown in Fig. 5(a), a third-order filter is displayed as an example. The third-order BPF are composed of three lines and three types of varactors. The varactor C_3 are utilized for the controllable and additional third pole in the passband.

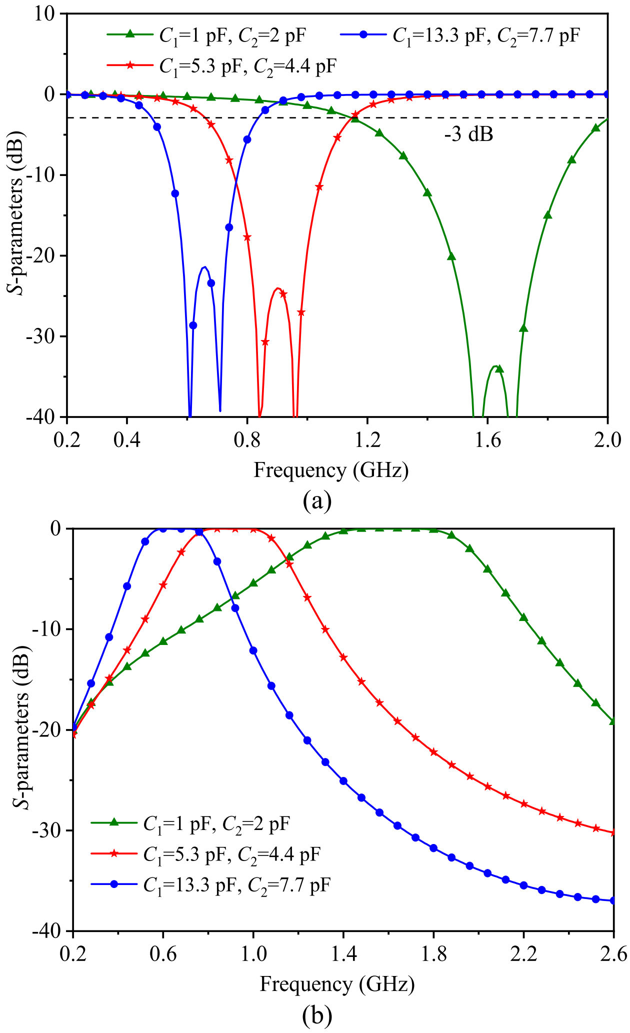

FIGURE 4. **The theoretical curves of the proposed tunable BPF. (a) $|S_{11}|$. (b) $|S_{21}|$.**

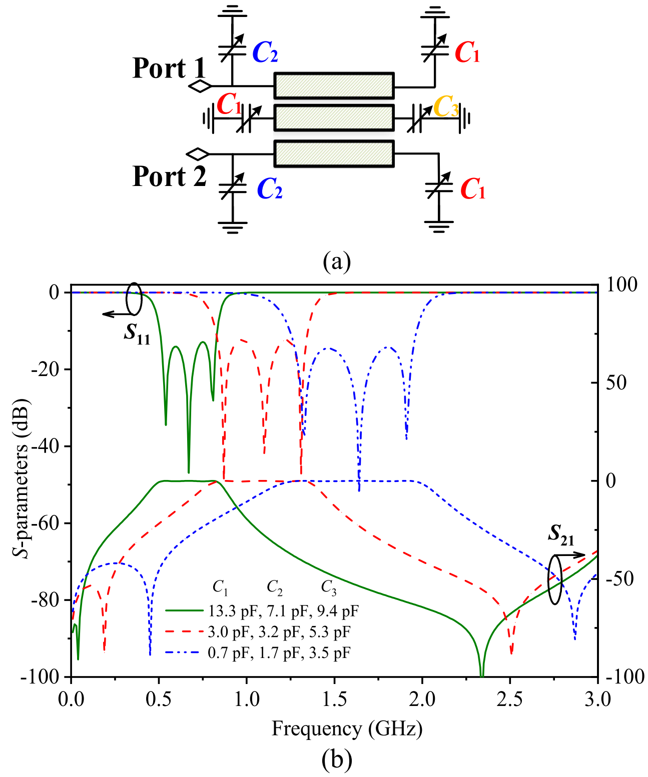

FIGURE 5. **(a) The proposed third-order tunable BPF. (The length, width, and the gap between the coupled lines are 29 mm, 0.5 mm, and 0.12 mm, respectively. The substrate is with a relative permittivity of 3.48, a loss tangent of 0.0037, and a thickness of 0.508 mm.) (b) The *S*-parameters of the third-order tunable BPF.**

Fig. 5(b) indicates the performances of the third-order filter. As the third-order tunable BPF, C_1 is mainly aimed to affect the center frequencies of any states, in the meantime, C_2 and C_3 determine the impedance matching and operating bandwidths.

III. SIMULATED AND MEASURED RESULTS

A. DESIGN AND SIMULATED RESULTS

In order to validate the design theory, an experimental structure is modeled by the full wave electromagnetic simulator ANSYS HFSS and the 3D structure of the proposed tunable BPF is shown in Fig. 6. The layout of the fabricated tunable BPF is shown in Fig. 7. The optimized physical dimensions of the design are demonstrated in TABLE 2.

Aimed at realizing the tunability through DC voltages, suitable bias circuits have to be designed and applicable lumped elements are required to be chosen. In simulation, the values of C_1 and C_2 are set at the range from 0.7 pF to 13.3 pF. Chip inductors and capacitors are used as radio frequency chokes (RFC) and DC blocks, respectively. Chip resistances are utilized for limiting current to avoid damaging the tunable capacitors. The length S_l reserved for the placement of chip components and varactors are 1.2 mm. The radius of via holes are 0.575 mm which is half the width of the microstrip line. DC voltages are equivalent to be shorted for radio frequency

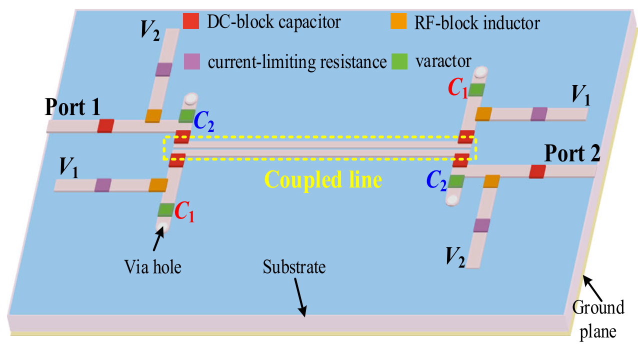

FIGURE 6. **The 3D structure of the proposed tunable BPF on the substrate of RO4350B.**

TABLE 2. **Dimensions of the fabricated tunable BPF.**

Parameters	L_1	L_2	L_3	L_4	L_5	W_c
Value (mm)	5	4	7.7	2	28.9	0.52
Parameters	S_c	W_d	L_p	W_p	h	S_l
Value (mm)	0.12	1.15	54.4	35	0.508	1.2

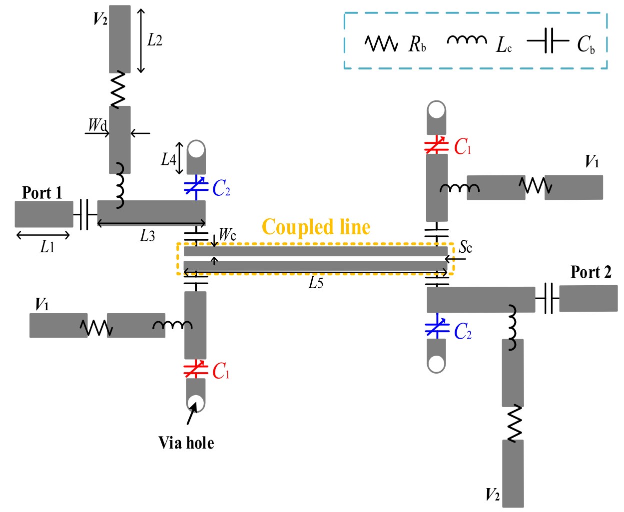

FIGURE 7. The layout of the fabricated tunable BPF.

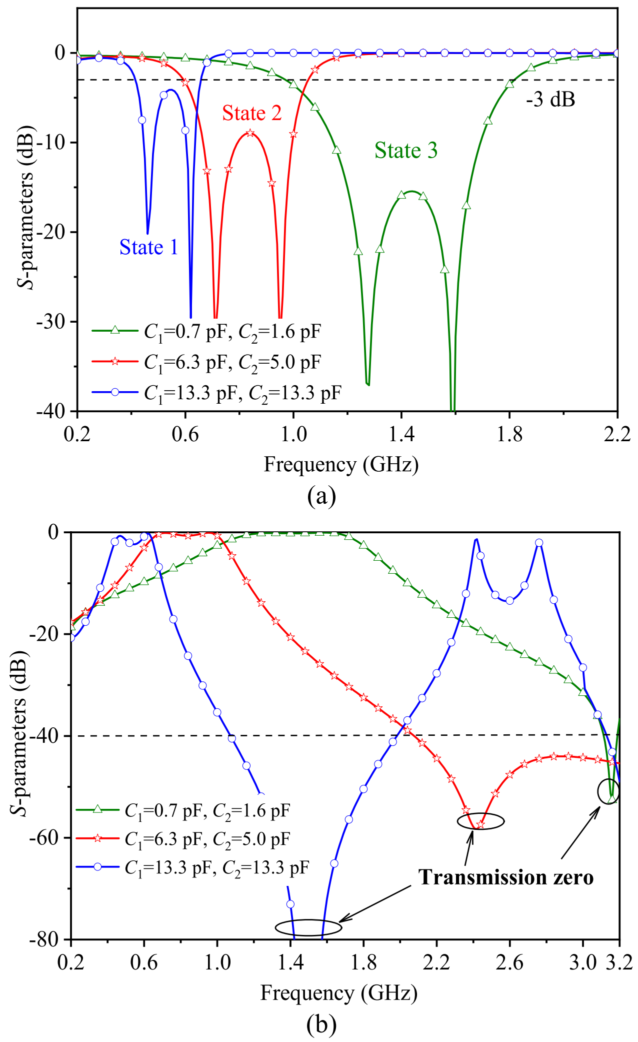

FIGURE 8. Simulated scattering parameters of the proposed tunable bandpass filter at three states. (a) $|S_{11}|$. (b) $|S_{21}|$.

signals, thus the bias voltages are shorted to the ground in simulations.

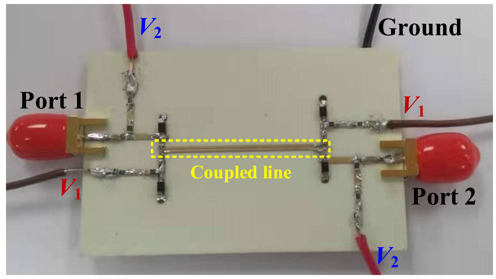

FIGURE 9. The photograph of the fabricated tunable BPF.

TABLE 3. Simulated and measured center frequency (f_c) and 3-dB bandwidth under three states.

	Center frequency (GHz)		3-dB ABW (MHz) /RBW	
	simulated	measured	simulated	measured
State 1	0.536	0.494	240 (44.78%)	282 (57.09%)
State 2	0.829	0.762	452 (54.52%)	549 (72.05%)
State 3	1.397	1.257	837 (59.91%)	943 (75.02%)
Tuning range	89.08%	87.15%	349%	334%

ABW: absolute bandwidth; RBW: relative bandwidth.

The simulated scattering parameters of the proposed tunable BPF at three states including $|S_{11}|$ and $|S_{21}|$ are shown in Fig. 8. It can be observed from Fig. 8(a) that when the tunable capacitors are $C_1 = 13.3$ pF and $C_2 = 13.3$ pF, the initial center frequency and 3-dB bandwidth of the design are 536 MHz and 240 MHz, respectively.

By regulating the values of the tunable capacitors, the tuning range accomplishes of tuning center frequency f_c from 536 MHz to 1.397 GHz and bandwidth from 240 MHz to 837 MHz. It should be noted that the simulated results of $|S_{21}|$ indicate that there occurs transmission zeros (TZs) at the edge of the upper band (Fig. 8(b)). Due to the addition of the DC-block capacitors placed between microstrip lines as well as the coupled line, and the necessary microstrip line at the end of coupled line for the placement of inductors and varactors, a TZ is generated under the range of the frequency researched in our study, compared with the ideal results in Fig. 4(b). In fact, a TZ exists at 3.3 GHz in the ideal simulation, while the available frequency responses are not shown, because such frequencies are outside the scope of the study. The arrangement of metal lines in printed circuit board (PCB) for actual test, principally the indispensable microstrip lines for radio frequency signals, results in the movement of the TZ.

B. IMPLEMENTATION AND MEASURED RESULTS

To verify the proposed design, a prototype operating at the center frequency f_0 of 1 GHz is fabricated and measured, as demonstrated in Fig. 9. The substrate RO4350B with a relative permittivity of 3.48, a size of $L_p \times W_p \times h$, and a loss tangent of 0.0037 is used for the tunable BPF.

TABLE 4. Comparisons of the proposed filter with other referenced prototypes.

Refs.	Center frequency tuning range (GHz)	BW tuning range (GHz)	Insertion loss (dB)	Bias voltages (V)	No. of varactors	Simple structure
[14]	0.97-1.72 (55.7%)	Constant ABW	3-4.5	≤14.6	4	No
[22]	0.56-1.15 (69%)	0.065-0.18 (277%) [a]	1.4-4.5	≤20	6	No
[11]	0.95-1.45 (41.7%)	0.08-0.1 (125%) [b]	<3	≤20	3	No
[12]	1.5-2.2 (37.84%)	0.05-0.17 (340%) [a]	<9.5	≤19	9	No
[13]	0.58-1.22 (71.1%)	0.065-0.18 (277%) [b]	1.8-4.6	≤26	12	No
This work	**0.494-1.257 (87.15%)**	**0.282-0.943 (334%) [b]**	**2.38-5.52**	**≤16**	**4**	**Yes**

ABW: absolute bandwidth; [a] 1dB bandwidth, [b] 3 dB bandwidth.

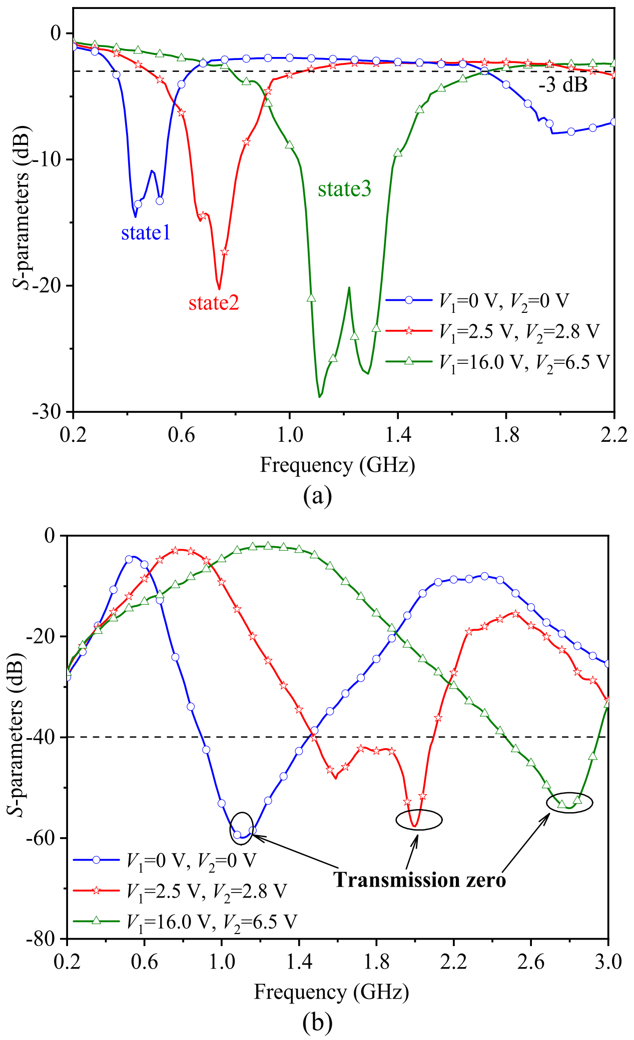

FIGURE 10. Measured scattering parameters of the designed fabricated tunable BPF. (a) $|S_{11}|$. (b) $|S_{21}|$.

The chosen values of lumped elements including DC-block capacitors C_b, RF-block inductors L_c, current-limiting resistances R_b, and varactors C_1 and C_2 (SMV1281-011LF SKYWORKS SOD323) [39] are listed as follows: C_b = 4.7 nF, L_c = 3.3 uH, R_b = 10 kΩ, and $C_1(C_2)$ = 0.69-13.30 pF. As demonstrated in [1], four DC-block capacitors C_b are adopted to isolate two tunable voltages, which are located between coupled line and microstrip line. In addition, two capacitors C_b are placed to eliminate the influence of DC voltages on ports. All S-parameter measurements are carried out by using R&S vector network analyzer ZVA-8.

Fig. 10 illustrates the measured return losses and transmission coefficients of the fabricated tunable BPF at three different states. Fig. 10 reveals that the 3-dB operating bandwidth extends from 282 MHz to 943 MHz, and center frequency f_c shifts from 494 MHz to 1.257 GHz. Specific tuning range of center frequency (f_c) and 3-dB bandwidth under three states in simulations and measurements are listed in TABLE 3. The operating bandwidths are increasing, as the center frequencies go up, as shown in TABLE 3. Due to the addition of DC-block capacitors C_b and gap capacitances, the equivalent capacitance loaded at the end of the coupled line are increased, which leads to the TZs shifting compared to simulation results.

Moreover, the measured return losses are better than 10 dB and the insertion losses are less than 5.52 dB, which are attributed to the loss of lumped elements and SMAs. Besides, the comparisons of the proposed filter with other referenced prototypes are summarized in TABLE 4. It can be seen that the proposed filter based on coupled line achieves a wider center frequency and bandwidth tuning range with only two relatively low bias voltages and 4 varactors.

IV. CONCLUSION

A tunable bandpass filter using coupled line with wide tuning range is demonstrated. By introducing four tunable capacitors into the coupled line, the operating center frequency and bandwidth can be easily controlled by bias voltages. A prototype of the design has been manufactured and experimented. The experimental results have presented that the proposed tunable BPF realizes wider tuning range, compared with other designs. Hence, it can be expected that the proposed design is potential to apply in wideband tunable devices.

REFERENCES

[1] X. Shen, Y. Wu, S. Zhou, and Y. Liu, "A novel coupled-line tunable Wilkinson power divider with perfect port match and isolation in wide frequency tuning range," *IEEE Trans. Compon., Packag., Manuf. Technol.*, vol. 6, no. 6, pp. 917–925, Jun. 2016.

[2] A. Chen, Y. Zhuang, J. Zhou, Y. Huang, and L. Xing, "Design of a broadband Wilkinson power divider with wide range tunable bandwidths by adding a pair of capacitors," *IEEE Trans. Circuits Syst. II, Exp. Briefs*, vol. 66, no. 4, pp. 567–571, Apr. 2019.

[3] M. E. Bialkowski and A. M. Abbosh, "Design of a compact UWB out-of-phase power divider," *IEEE Microw. Wireless Compon. Lett.*, vol. 17, no. 4, pp. 289–291, Apr. 2007.

[4] A. M. Abbosh, "Compact tunable reflection phase shifters using short section of coupled lines," *IEEE Trans. Microw. Theory Techn.*, vol. 60, no. 8, pp. 2465–2472, Aug. 2012.

[5] B. An, G. Chaudhary, and Y. Jeong, "Wideband tunable phase shifter with low in-band phase deviation using coupled line," *IEEE Microw. Wireless Compon. Lett.*, vol. 28, no. 8, pp. 678–680, Aug. 2018.

[6] A. M. Abbosh, "Tunable phase shifter employing variable odd-mode impedance of short-section parallel-coupled microstrip lines," *IET Microw., Antennas Propag.*, vol. 6, no. 3, pp. 305–311, 2012.

[7] W. J. Liu, S. Y. Zheng, Y. M. Pan, Y. X. Li, and Y. L. Long, "A wide-band tunable reflection-type phase shifter with wide relative phase shift," *IEEE Trans. Circuits Syst. II, Exp. Briefs*, vol. 64, no. 12, pp. 1442–1446, Dec. 2017.

[8] P.-L. Chi and T.-C. Hsu, "Highly reconfigurable quadrature coupler with ideal impedance matching and port isolation," *IEEE Trans. Microw. Theory Techn.*, vol. 65, no. 8, pp. 2930–2941, Aug. 2017.

[9] B. W. Xu, S. Y. Zheng, W. M. Wang, Y. L. Wu, and Y. A. Liu, "A coupled line-based coupler with simultaneously tunable phase and frequency," *IEEE Trans. Circuits Syst. I, Reg. Papers*, vol. 66, no. 12, pp. 4637–4647, Dec. 2019.

[10] Y. F. Pan, S. Y. Zheng, Y. M. Pan, Y. X. Li, and Y. L. Long, "Highly reconfigurable dual-band coupler with independently tunable operating frequencies," *IEEE Trans. Ind. Electron.*, vol. 66, no. 5, pp. 3615–3626, May 2019.

[11] C.-W. Tang, C.-T. Tseng, and S.-C. Chang, "A tunable bandpass filter with modified parallel-coupled line," *IEEE Microw. Wireless Compon. Lett.*, vol. 23, no. 4, pp. 190–192, Apr. 2013.

[12] Y.-C. Chiou and G. M. Rebeiz, "A tunable three-pole 1.5–2.2-GHz bandpass filter with bandwidth and transmission zero control," *IEEE Trans. Microw. Theory Techn.*, vol. 59, no. 11, pp. 2872–2878, Nov. 2011.

[13] H. Zhu and A. M. Abbosh, "Tunable balanced bandpass filter with wide tuning range of center frequency and bandwidth using compact coupled-line resonator," *IEEE Microw. Wireless Compon. Lett.*, vol. 26, no. 1, pp. 7–9, Jan. 2016.

[14] K. Song, X. Wang, M. Fan, Y. Chen, S. R. Patience, A. M. Iman, and Y. Fan, "Tunable balanced bandpass filter with constant absolute bandwidth and high common mode suppression," *IET Microw., Antennas Propag.*, vol. 14, no. 2, pp. 147–152, Feb. 2020.

[15] W.-J. Zhou and J.-X. Chen, "High-selectivity tunable balanced bandpass filter with constant absolute bandwidth," *IEEE Trans. Circuits Syst. II, Exp. Briefs*, vol. 64, no. 8, pp. 917–921, Aug. 2017.

[16] Y.-C. Chiou and G. M. Rebeiz, "A quasi elliptic function 1.75–2.25 GHz 3-pole bandpass filter with bandwidth control," *IEEE Trans. Microw. Theory Techn.*, vol. 60, no. 2, pp. 244–249, Feb. 2012.

[17] J.-R. Mao, W.-W. Choi, K.-W. Tam, W. Q. Che, and Q. Xue, "Tunable bandpass filter design based on external quality factor tuning and multiple mode resonators for wideband applications," *IEEE Trans. Microw. Theory Techn.*, vol. 61, no. 7, pp. 2574–2584, Jul. 2013.

[18] C.-W. Tang, C.-T. Tseng, and S.-C. Chang, "Design of the compact tunable filter with modified coupled lines," *IEEE Trans. Compon., Packag., Manuf. Technol.*, vol. 4, no. 11, pp. 1815–1821, Nov. 2014.

[19] H. Joshi, H. H. Sigmarsson, S. Moon, D. Peroulis, and W. J. Chappell, "High-*Q* fully reconfigurable tunable bandpass filters," *IEEE Trans. Microw. Theory Techn.*, vol. 57, no. 12, pp. 3525–3533, Dec. 2009.

[20] P. Kim and Y. Jeong, "A new synthesis and design approach of a complex termination impedance bandpass filter," *IEEE Trans. Microw. Theory Techn.*, vol. 67, no. 6, pp. 2346–2354, Jun. 2019.

[21] J.-X. Chen, Y.-J. Zhang, J. Cai, Y.-L. Li, and Y.-J. Yang, "Overall study of frequency-agile mechanism of varactor-loaded λ/4 resonator for designing tunable filter with stable wide stopband," *IEEE Trans. Ind. Electron.*, vol. 66, no. 8, pp. 6302–6310, Aug. 2019.

[22] G. Zhang, Y. Xu, and X. Wang, "Compact tunable bandpass filter with wide tuning range of centre frequency and bandwidth using short coupled lines," *IEEE Access*, vol. 6, pp. 2962–2969, 2018.

[23] J. Long, C. Li, W. Cui, J. Huangfu, and L. Ran, "A tunable microstrip bandpass filter with two independently adjustable transmission zeros," *IEEE Microw. Wireless Compon. Lett.*, vol. 21, no. 2, pp. 74–76, Feb. 2011.

[24] D. Lu, M. Yu, N. S. Barker, Z. Li, W. Li, and X. Tang, "Advanced synthesis of wide-tuning-range frequency-adaptive bandpass filter with constant absolute bandwidth," *IEEE Trans. Microw. Theory Techn.*, vol. 67, no. 11, pp. 4362–4375, Nov. 2019.

[25] L. Gao, T.-W. Lin, and G. M. Rebeiz, "Design of tunable multi-pole multi-zero bandpass filters and diplexer with high selectivity and isolation," *IEEE Trans. Circuits Syst. I, Reg. Papers*, vol. 66, no. 10, pp. 3831–3842, Oct. 2019.

[26] H.-Y. Tsai, T.-Y. Huang, and R.-B. Wu, "Varactor-tuned compact dual-mode tunable filter with constant passband characteristics," *IEEE Trans. Compon., Packag., Manuf. Technol.*, vol. 6, no. 9, pp. 1399–1407, Sep. 2016.

[27] C. H. Kim and K. Chang, "Ring resonator bandpass filter with switchable bandwidth using stepped-impedance stubs," *IEEE Trans. Microw. Theory Techn.*, vol. 58, no. 12, pp. 3936–3944, Dec. 2010.

[28] S. Fouladi, F. Huang, W. D. Yan, and R. R. Mansour, "High-*Q* narrowband tunable combline bandpass filters using MEMS capacitor banks and piezomotors," *IEEE Trans. Microw. Theory Techn.*, vol. 61, no. 1, pp. 393–402, Jan. 2013.

[29] A. Miller and J.-S. Hong, "Wideband bandpass filter with reconfigurable bandwidth," *IEEE Microw. Wireless Compon. Lett.*, vol. 20, no. 1, pp. 28–30, Jan. 2010.

[30] R. Lababidi, M. Al Shami, M. Le Roy, D. Le Jeune, K. Khoder, and A. Pérennec, "Tunable channelised bandstop passive filter using reconfigurable phase shifter," *IET Microw., Antennas Propag.*, vol. 13, no. 5, pp. 591–596, Apr. 2019.

[31] Y.-C. Ou and G. M. Rebeiz, "Lumped-element fully tunable bandstop filters for cognitive radio applications," *IEEE Trans. Microw. Theory Techn.*, vol. 59, no. 10, pp. 2461–2468, Oct. 2011.

[32] J. Ni and J. Hong, "Compact continuously tunable microstrip low-pass filter," *IEEE Trans. Microw. Theory Techn.*, vol. 61, no. 5, pp. 1793–1800, May 2013.

[33] J. Ni and J. Hong, "Compact varactor-tuned microstrip high-pass filter with a quasi-elliptic function response," *IEEE Trans. Microw. Theory Techn.*, vol. 61, no. 11, pp. 3853–3859, Nov. 2013.

[34] L. Guo, H. Zhu, and A. Abbosh, "Phase reconfigurable microwave power divider," *IEEE Trans. Circuits Syst. II, Exp. Briefs*, vol. 66, no. 1, pp. 21–25, Jan. 2019.

[35] Y. Wu, Y. Liu, S. Li, and S. Li, "A novel high-power amplifier using a generalized coupled-line transformer with inherent DC-block function," *Prog. Electromagn. Res.*, vol. 119, pp. 171–190, 2011.

[36] Y. Wu, Y. Liu, S. Li, and C. Yu, "New coupled-line dual-band DC-block transformer for arbitrary complex frequency-dependent load impedance," *Microw. Opt. Technol. Lett.*, vol. 54, no. 1, pp. 139–142, Jan. 2012.

[37] X. Tan and F. Lin, "A novel rat-race coupler with widely tunable frequency," *IEEE Trans. Microw. Theory Techn.*, vol. 67, no. 3, pp. 957–967, Mar. 2019.

[38] J.-S. Row and M.-J. Hou, "Design of polarization diversity patch antenna based on a compact reconfigurable feeding network," *IEEE Trans. Antennas Propag.*, vol. 62, no. 10, pp. 5349–5352, Oct. 2014.

[39] *Data Sheet-SMV1281 Series: Hyperabrupt Junction Tuning Varactors*, Skyworks Solutions Inc., Woburn, MA, USA, 2015.

[40] Y.-H. Cho, and G. M. Rebeiz, "Two- and four-pole tunable 0.7–1.1-GHz bandpass-to-bandstop filters with bandwidth control," *IEEE Trans. Microw. Theory Techn.*, vol. 62, no. 3, pp. 457–463, Mar. 2014.

[41] X.-G. Wang, Y.-H. Cho, and S.-W. Yun, "A tunable combline bandpass filter loaded with series resonator," *IEEE Trans. Microw. Theory Techn.*, vol. 60, no. 6, pp. 1569–1576, Jun. 2012.

XIAOXIAO CHEN received the B.S. degree in electronic information engineering from the Ocean University of China (OUC), Qingdao, China, in 2018. She is currently pursuing the M.S. degree with the School of Electronic Engineering, Beijing University of Posts and Telecommunications (BUPT), Beijing, China. Her research interests include graphene-based antennas and tunable microwave components.

YONGLE WU (Senior Member, IEEE) received the B.Eng. degree in communication engineering and the Ph.D. degree in electronic engineering from the Beijing University of Posts and Telecommunications (BUPT), Beijing, China, in 2006 and 2011, respectively.

From April 2010 to October 2010, he was a Research Assistant with the City University of Hong Kong (CityU), Kowloon, Hong Kong. In 2011, he joined BUPT, where he is currently a Full Professor with the School of Electronic Engineering. His research interests include microwave components, circuits, antennas, and wireless systems design.

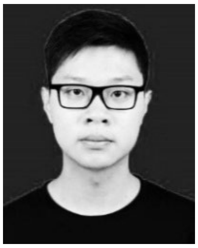

YUHAO YANG received the B.Eng. degree in communication engineering from the Xi'an University of Science and Technology (XUST), Xi'an, China, in 2018. He is currently pursuing the M.S. degree with the Beijing University of Posts and Telecommunications (BUPT), Beijing, China.

In September 2018, he started his research as a Graduate with BUPT. His research interests include microwave passive components, integrated passive device (IPD) technology, and multiband impedance transformers.

WEIMIN WANG (Member, IEEE) received the B.S. degree in communication engineering, the M.S. degree in electromagnetic field and microwave technology, and the Ph.D. degree in electronic science and technology from the Beijing University of Posts and Telecommunications (BUPT), Beijing, China, in 1999, 2004, and 2014, respectively. In 2014, she joined BUPT, where she is currently an Associate Professor with the School of Electronic Engineering. Her research interests include electromagnetic field, microwave circuits, antennas, and MIMO OTA measurement.